The Microwave Spectrum of trans-2,3-Dimethyloxirane in Torsional Excited States

H. Hartwig and H. Dreizler

Institut für Physikalische Chemie, Christian-Albrechts-Universität zu Kiel, Olshausenstr. 40, D-24098 Kiel

Z. Naturforsch. **51a**, 923–932 (1996); received May 2, 1996

The microwave spectrum of trans-2,3-dimethyloxirane ($CH_3CHOCHCH_3$) in the excited torsional states $v_{17} = 1$ and $v_{33} = 1$ has been measured in the range from 8 to 26 GHz and assigned. An analysis of internal rotation splittings of the observed rotational transitions was performed using the internal axis method (or "combined axis method") with a newly developed program accounting for the top-top coupling. The threefold hindering potential V_3 and the direction cosines $\lambda_{g,i}$ of the internal rotation axes i with respect to the principal inertia axes g are in a good agreement with the ground state values. Additionally, the sixfold hindering parameter V_6 was found to be $-0.2600(12)$ kJ/mol. The value of the parameter V'_{12} describing the top-top coupling in the potential function (via $V'_{12} \sin 3\tau_1 \sin 3\tau_2$), was determined to $-0.4240(6)$ kJ/mol.

Introduction

The vibrational ground state microwave spectrum of trans-2,3-dimethyloxirane (trans-epoxy-butane, "TEB") was first assigned by Emptage in 1967 [1]. He was able to determine the threefold barrier to internal rotation V_3 of the two methyl groups, yielding a value of 2444(150) cal/mol (10.216(627) kJ/mol). Further investigations [2] utilized the high resolution of molecular beam Fourier transform microwave spectroscopy [3, 4]. With these precise measurements the value for V_3 was improved, additionally the moment of inertia $I_{\tau,i}$ of the methyl group i and the angles between the torsion axis and the principal axes of inertia g were determined by an analysis of the internal rotation splittings. The angle τ_i labels the internal rotation of the top i, in the literature also often denoted as α.

As Emptage pointed out, TEB is a test molecule to study the interaction between the two methyl groups, because it can be easily compared with methyloxirane (propenoxid, CH_3CHOCH_2) and cis-2,3-dimethyloxirane. It turns out that the internal rotation barrier V_3 of TEB is quite similar to the one of methyloxirane (10.71(29) kJ/mol), but the barrier of cis-2,3-dimethyloxirane (6.89(2) kJ/mol) is significantly lower. The reason for this change is explained by a different top-top interaction according to the different steric positions of the methyl groups. The similar values of the barrier V_3 in TEB and methyloxirane, were no top-top coupling appears, supports the expectation that the top-top coupling in TEB is relatively small.

In order to obtain direct information about the coupling between the two methyl groups, the ground state measurements are not sufficient. Durig and coworkers [5] recorded IR- and Raman spectra of TEB and presented a vibrational analysis. They were able to verify the value of the potential barrier V_3 as obtained from microwave spectroscopy, furthermore they determined the potential parameters V_6 and V'_{12}. In this paper we present the analysis of the rotational spectrum of trans-2,3-dimethyloxirane in the symmetric and antisymmetric torsional modes $v_{17} = 1$ and $v_{33} = 1$. The simultaneous fit of both states allows to determine the potential parameters V'_{12} [6]. This potential parameter describes the energy difference between the v_{17} and v_{33} states, together with a kinetic term proportional to F_{12} in the Hamiltonian given below.

Furthermore, we describe the theoretical background for the analysis of the internal rotation splittings by means of the so called "internal axis method" as given by Woods [7, 8]. To avoid confusion with the "internal axis method" of Nielsen [9] for molecules with one internal rotor, we refer to the method used as the "combined axis method" (CAM).

Hamiltonian

The Hamiltonian for a molecular model consisting of a rigid asymmetric frame and two rigid symmetric

Reprint requests to Prof. Dr. H. Dreizler.

0932-0784 / 96 / 0800-0923 $ 06.00 © – Verlag der Zeitschrift für Naturforschung, D-72072 Tübingen

internal rotors is given by several authors, e.g. [6, 10, 11]. We will use the form

$$\hat{H} = \hat{H}_{rr} + \hat{H}_1 + \hat{H}_2 + \hat{H}_{12}\,. \tag{1}$$

The rigid rotor part $\hat{H}_{rr}$ contains the structural moments of inertia

$$\hat{H}_{rr} = \tfrac{1}{2}\,\hat{\mathbf{P}}^{\top}\mathbf{I}^{-1}\,\hat{\mathbf{P}} \tag{2}$$

with the angular momentum operator $\hat{\mathbf{P}}^{\top} = (\hat{P}_x, \hat{P}_y, \hat{P}_z)$ and the tensor of inertia $\mathbf{I}$. The $^{\top}$ symbol denotes a transposed matrix. The operators $\hat{H}_1$ and $\hat{H}_2$ result from the internal rotation of one top and include all crossterms between overall and internal rotation (*Coriolis*-coupling):

$$\hat{H}_i = F_{ii}(\hat{p}_i - \boldsymbol{\varrho}_i^{\top}\hat{\mathbf{P}})^2 + \frac{V_{3,i}}{2}(1 - \cos 3\tau_i) + \frac{V_{6,i}}{2}(1 - \cos 6\tau_i)\,. \tag{3}$$

The angle τ_i describes the torsion of the top i ($i = 1, 2$) relative to the frame, the operator $\hat{p}_i$ is the angular momentum operator $\hat{p}_i = -i\partial/\partial\tau_i$ of the internal rotation. The value of $\hbar$ is absorbed in the kinetic parameters $\mathbf{I}^{-1}$ and F_{ii}, where F_{ii} ($i = 1, 2$) is considered as a rotational constant of the torsional motion.

The last part $\hat{H}_{12}$ is responsible for the top-top interaction of a molecule with C_2 symmetry:

$$\begin{aligned}\hat{H}_{12} = {} & F_{12}[(\hat{p}_1 - \boldsymbol{\varrho}_1^{\top}\hat{\mathbf{P}})(\hat{p}_2 - \boldsymbol{\varrho}_2^{\top}\hat{\mathbf{P}}) \\ & + (\hat{p}_2 - \boldsymbol{\varrho}_2^{\top}\hat{\mathbf{P}})(\hat{p}_1 - \boldsymbol{\varrho}_1^{\top}\hat{\mathbf{P}})] \\ & + V_{12}\cos 3\tau_1 \cos 3\tau_2 + V'_{12}\sin 3\tau_1 \sin 3\tau_2 \\ & + V''_{12}(\sin 3\tau_1 \cos 3\tau_2 + \cos 3\tau_1 \sin 3\tau_2)\,.\end{aligned} \tag{4}$$

The vector $\boldsymbol{\varrho}_i$ of the i-th top is defined by

$$\boldsymbol{\varrho}_i = \mathbf{I}^{-1}\boldsymbol{x}_i\,, \quad \boldsymbol{x}_i = I_{\tau,i}\boldsymbol{\lambda}_i\,, \tag{5}$$

where $\boldsymbol{\lambda}_i$ is a vector of unit length parallel to the internal rotation axis. The components λ_x, λ_y and λ_z are direction cosines, they are often (especially in the PAM) important parameters in the fit. $I_{\tau,i}$ is the moment of inertia of the top i. The elements $F_{i,i'}$ of the matrix $\mathbf{F}$ are given as

$$2\mathbf{F} = (\mathbf{Y} - \mathbf{X}^{\top}\mathbf{I}^{-1}\mathbf{X})^{-1}, \quad Y_{i,i} = I_{\tau,i} \quad \text{and} \quad Y_{i,i'} = 0\,, \quad i \neq i'\,. \tag{6}$$

The matrix $\mathbf{X}$ is a 3×2 matrix built from the column vectors $\boldsymbol{x}_1$ and $\boldsymbol{x}_2$ in the following way: $\mathbf{X} = (\boldsymbol{x}_1, \boldsymbol{x}_2)$. It should be noted that the formulas in this chapter are not related to a specific coordinate system.

Coordinate System

The Hamiltonian (1) is known for a long time and several methods for the numerical treatment are proposed in the literature [12]. Closely correlated is the choice of coordinate systems; the principal axis and the internal axis methods (PAM and IAM) are often discussed in this context. In the case of one internal rotor, Hougen et al. [13] pointed out three useful ways of defining a molecule oriented coordinate system: (i) the principal inertial axis system. Its position refered to the rigid frame and rigid top molecular model is invariant to internal rotation as the top is assumed to be symmetric. (ii) The internal axis system, initially described by Nielsen [9], rotates with respect to the frame as well as to the top in a way, that no coupling between the torsional motion and the overall rotation occurs explicitly. On the other hand the elements of the tensor of inertia become dependent on the torsional angle τ, the boundary conditions for the eigenvalues are modified. (iii) The "rho axis system" is fixed in the molecular frame but is orientated with respect to the internal rotation axis of the top. Choosing the z' axis of a new coordinate system collinear with the vector $\boldsymbol{\varrho}$, only coupling between the internal rotation angular momentum $\hat{p}_i$ and $\hat{P}_{z'}$, the component of the overall angular momentum, remains. We call the method based on this coordinate choice "rho axis method" (RAM).

For two internal rotors the situation is different. In a general case it not possible to find a coordinate system where the angular momenta of both internal motions vanish simultaneously. If the two tops and the internal rotation barriers were different, one could think of appling these techniques for one top (IAM or RAM) to the top with the strongest coupling, but the other top has to be treated without any simplifications.

Because in TEB and other molecules both tops are equivalent, it is desirable to use a theoretical treatment which respects this equality. Here the principal axis system is the convenient choice for an initial coordinate system. Consequently the moments of inertia can be obtained most easily. It should be noted that several authors used the idiom IAM for a special technique first introduced by Woods [8] to calculate the spectrum of molecules with two or more symmetric internal rotors. In spite of the name IAM, this method also uses the principal axis system in the last step of the calculation. To avoid this ambiguity of the idiom

IAM, we will refer to the method of Woods as the *Combined Axes Method* (CAM) because its utilizes a combination of several different coordinate systems during the calculation. For each top a separate rho axis system is defined and eigenvalues of an adapted part of the Hamiltonian connected with the internal rotation of this top are calculated. Finally the eigenvalues in the initial principal axis system are determined. Details are given below.

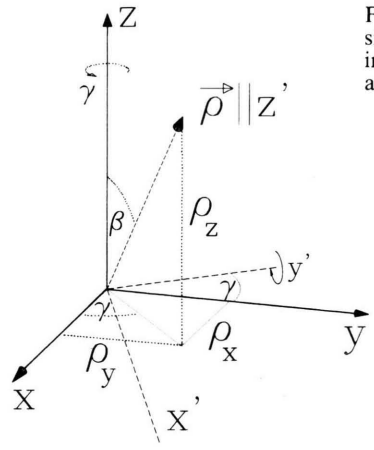

Fig. 1. Schematic position of the vector $\boldsymbol{\varrho}$ in the principal inertia axis system x, y, z.

Numerical Solutions

To obtain eigenvalues of the Hamiltonian (1), several methods are discussed in literature. The oldest technique utilizes a van Vleck transformation, as described in [11] and [14]. This method has also been applied to analyze torsional excited states of two-top molecules [15].

Another approach which became suitable with increasing computer capability was based on the numerical diagonalization of a truncated Hamiltonian matrix [16]. The applied basisfunctions are products of suitable rotational and torsional functions. The extension of the method to excited states was presented by Meyer [17], he also used a K dependent prediagonalization scheme to reduce the size of the matrices.

A third method was introduced by Woods [7, 8] and later extended by Vacherand et al. [18]. This method is traditionally called IAM, but we will use the notation "CAM" to distinguish it from the coordinate system introduced by Nielsen [9]. Even though Woods gave theoretical formulas to include the two-top interaction operators which are necessary to calculate the torsional excited states, only ground state transition have been analyzed with this technique so far. We have implemented these operators in a program XIAM [19]. As a result we were able to fit the torsional excited states of TEB using the CAM technique.

In the CAM the main coordinate system is the principal axis system of the rigid frame rigid top molecule. Therefore, the Hamiltonian H_{rr} is straightforward:

$$\hat{H}_{rr} = B_x \hat{P}_x^2 + B_y \hat{P}_y^2 + B_z \hat{P}_z^2, \quad B_g = \hbar^2/2 I_g . \quad (7)$$

The Hamiltonian $\hat{H}_i$ for one internal rotor ($i = 1, 2$) is given in a different way. Because each internal rotor is treated independently, we will omit the index i in the next section. The following procedure must be carried out for each top successively.

Starting in the principal axis system, a contact transformation using the rotation operator $\hat{D}$ is performed to eliminate the $\varrho_x \hat{P}_x \hat{p}$ and $\varrho_y \hat{P}_y \hat{p}$ Coriolis coupling terms. This contact transformation has its geometrical equivalent in a rotation of the coordinate system. In the rotated system the z' axis is aligned parallel to the vector $\boldsymbol{\varrho}$, where $\boldsymbol{\varrho}$ is a vector fixed in the frame of the molecule (Figure 1). This rho axis system is described in [13]. The rotation is accomplished with the Euler angles β and γ,

$$\cos\gamma = \varrho_x (\varrho_x^2 + \varrho_y^2)^{-0.5}, \quad \cos\beta = \varrho_z (\varrho)^{-1} \quad (8)$$

with the components ϱ_g in the principal axis system. The scalar $\varrho = \sqrt{\varrho_x^2 + \varrho_y^2 + \varrho_z^2}$ gives the length of $\boldsymbol{\varrho}$.

$$\boldsymbol{\varrho}' = \mathbf{D}(\beta, \gamma)\,\boldsymbol{\varrho}, \quad \boldsymbol{\varrho} = (\varrho_x, \varrho_y, \varrho_z)^\top, \quad \boldsymbol{\varrho}' = (0, 0, \varrho)^\top . \quad (9)$$

Primed variables (e.g. $\boldsymbol{\varrho}'$) designate the rotated coordinate system. The rotation matrix $\mathbf{D}(\beta, \gamma)$ is given by

$$\mathbf{D}(\beta, \gamma) = \begin{pmatrix} \cos\beta & 0 & -\sin\beta \\ 0 & 1 & 0 \\ \sin\beta & 0 & \cos\beta \end{pmatrix} \begin{pmatrix} \cos\gamma & \sin\gamma & 0 \\ -\sin\gamma & \cos\gamma & 0 \\ 0 & 0 & 1 \end{pmatrix}. \quad (10)$$

Here, the third Euler angle α is not used, we fix it to zero. Thereby, the Euler coordinates degenerate to polar coordinates or, in terms of operators, the rotation is performed by the operator

$$\hat{D} = \exp(-i\beta \hat{P}_y) \exp(-i\gamma \hat{P}_z) .$$

In a second step, the opposite transformation $\hat{D}^{-1}$ must be accomplished to retain $\hat{H}$ in the principal axis system. This leads to

$$\hat{H}_i = \hat{D}^{-1} \hat{D} \hat{H}_i \hat{D}^{-1} \hat{D} \quad \text{with} \quad \hat{D}^{-1} \hat{D} = 1 \quad (11)$$

with

$$\hat{H}_i' = \hat{D}\,\hat{H}_i\,D^{-1} = F_{ii}(\hat{p}_i + \varrho_i \hat{P}_{z'})^2 + V(\tau_i)\,. \quad (12)$$

The Hamiltonian $\hat{H}_i$ in the principal axis system can be now written by means of the polar coordinates ϱ, β and γ:

$$\hat{H}_i = (\hat{D}(\beta,\gamma))^{-1}\,\hat{H}_i'(\varrho)\,\hat{D}(\beta,\gamma)\,. \quad (13)$$

The eigenvalues of (12) can be calculated conveniently, because all matrix elements are diagonal in the rotational quantum number K. Using the free rotor functions for the torsional part and the symmetric rotor functions $|JMK\rangle$, one obtains the eigenvalues $E_{K v\sigma,i}$ and the eigenfunctions $|JMKv_K\sigma,i\rangle$, where v_K is the torsional quantum number of a state depending on the value of K, and σ labels the torsional symmetry of one top (A or E). Because K is still a good quantum number, the τ_i dependent basis functions can be factored in the following way: (14)

$$\langle\phi\,\theta\,\chi\,\tau_i|JMKv_K\sigma,i\rangle = \langle\phi\,\theta\,\chi|JMK\rangle\langle\tau_i|v_K\sigma,i\rangle\,.$$

The angles ϕ, θ, and χ are the Euler angles describing the rotation of the whole molecule in space. The torsional part of the eigenfunctions is sometimes written as $|Kv\sigma,i\rangle$ [7], but we prefer to write K as an index here. Because external electric or magnetic fields will not be considered here, the M quantum number will be omitted now.

The basis functions for the total Hamiltonian $\hat{H}$ Eq.(1) are the product of the symmetric rotor functions $|JK\rangle$ and the K dependent torsional functions $|v_K\sigma,1\rangle|v_K\sigma,2\rangle$ of each top. The matrix elements of $\hat{H}_i$ in the principal axis system are calculated by transforming the eigenvalue matrix of $\hat{H}_i'$ obtained in the rho axis system, where it is diagonal, back to the principal axis system. This is shown here for the first top ($i=1$):

$$\begin{aligned}
&\langle JK|\langle v_K\sigma,1|\langle v_K\sigma,2|\hat{H}_1|JK'\rangle|v'_{K'}\sigma,1\rangle|v'_{K'}\sigma,2\rangle\\
&\quad=\langle v_K\sigma,2|v'_{K'}\sigma,2\rangle\sum_{v'',K'',v''',K'''}\\
&\quad\cdot\langle JKv_K\sigma,1|\hat{D}_1^{-1}|JK''v''_{K''}\sigma,1\rangle\\
&\quad\cdot\langle JK''v''_{K''}\sigma,1|\hat{H}_1'|JK'''v'''_{K'''}\sigma,1\rangle\\
&\quad\cdot\langle JK'''v'''_{K'''}\sigma,1|\hat{D}_1|JK'v'_{K'}\sigma,1\rangle\\
&\quad=\langle v_K\sigma,2|v'_{K'}\sigma,2\rangle\sum_{v'',K''}\langle v_K\sigma,1|v''_{K''}\sigma,1\rangle\\
&\quad\cdot\langle JK|\hat{D}_1^{-1}|JK''\rangle\cdot E_{K''v''\sigma,1}\langle v''_{K''}\sigma,1|v'_{K'}\sigma,1\rangle\\
&\quad\cdot\langle JK''|\hat{D}_1|JK'\rangle\,. \qquad (15)
\end{aligned}$$

The matrix elements $\langle JK|\hat{D}_i|JK'\rangle$ of the rotation operator (rotating z into z') are

$$\begin{aligned}
\langle JK|\hat{D}_i|JK'\rangle &= \langle JK|\hat{d}(\alpha_i)\hat{d}(\beta_i)\hat{d}(\gamma_i)|JK'\rangle\\
&=\exp(-i\alpha_i K)\,d^{(J)}_{KK'}(\beta_i)\exp(-i\gamma_i K')\,. \quad (16)
\end{aligned}$$

As noted above, the angle α is set to zero, but α would cancel out in (15) anyway. The values of $d^{(J)}_{KK'}(\beta)$ are tabulated for some low J values [20], they can be calculated in a recursive way starting from the $d^{(1)}(\beta)$ matrix using Clebsch-Gordan coefficients [7].

The matrix elements of the top-top interaction operator $\hat{H}_{12}$ can be derived in a similar manner. First, it is necessary to calculate the matrix elements of $(\hat{p}_i - \varrho_i\hat{P}_{z'})$, $\sin(3\tau_i)$, and $\cos(3\tau_i)$ numerically in their own rho axis system. They are diagnonal in K, but have off-diagonal elements in v. Then, they are transformed into the principal axis system analogous to the above procedure (15):

$$\begin{aligned}
O_{JKK'vv'\sigma,i} &= \sum_{v'',K'',v''',K'''}\langle v_K\sigma,i|v''_{K''}\sigma,i\rangle\\
&\cdot\langle JK|\hat{D}_i^{-1}|JK''\rangle\,O'_{K''v''v'''\sigma,i}\,\delta_{K''',K'''}\\
&\cdot\langle v'''_{K'''}\sigma,i|v'_{K'}\sigma,i\rangle\,\langle JK'''|\hat{D}_i|JK'\rangle\,. \quad (17)
\end{aligned}$$

In (17), $O_{JKK'vv'\sigma,i}$ represents a matrix element of one top (e.g. $\hat{p}_1$) in the principal axis system, whereas $O'_{Kvv'\sigma,i}$ stands for an element in the rho axis system. The matrix elements of a product of two operators $\hat{O}_1\hat{O}_2$ of different tops are

$$\begin{aligned}
&\langle JK|\langle v_K\sigma,1|\langle v_K\sigma,2|\hat{O}_1\hat{O}_2|JK'\rangle|v'_{K'}\sigma,1\rangle|v'_{K'}\sigma,2\rangle\\
&\quad=\sum_{K''}\langle JK|\langle v_K\sigma,1|\hat{O}_1|v'_{K''}\sigma,1\rangle|JK''\rangle\\
&\quad\cdot\langle JK''|\langle v_{K''}\sigma,2|\hat{O}_2|v'_{K'}\sigma,2\rangle|JK'\rangle\\
&\quad=\sum_{K''}O_{JKK''vv'\sigma,1}\,O_{JK''K'vv'\sigma,2}\,. \qquad (18)
\end{aligned}$$

Finally, the matrix elements of the rigid rotor part $\hat{H}_{rr}$ are (19)

$$\begin{aligned}
&\langle JK|\langle v_K\sigma,1|\langle v_K\sigma,2|\hat{H}_{rr}|JK'\rangle|v'_{K'}\sigma,1\rangle|v'_{K'}\sigma,2\rangle\\
&=\langle v_K\sigma,1|v'_{K'}\sigma,1\rangle\langle v_K\sigma,2|v'_{K'}\sigma,2\rangle\langle JK|\hat{H}_{rr}|JK'\rangle\,.
\end{aligned}$$

The energy matrix of the complete Hamiltonian (1) is the sum of matrix elements of the rigid rotor part, of the transformed eigenvalues of each top (15) and of the matrix elements of the two-top operator $\hat{H}_{12}$ as shown in (18).

The numerical advantage of this CAM treatment is the fact, that the off-diagonal matrix elements in v generated by the operators $\hat{H}_{rr}$ and $\hat{H}_i$ can be neglected. This results from properties of the torsional

integrals $\langle v_K \sigma, i | v'_{K'} \sigma, i\rangle$ in the high barrier limit [21]. The quantity s_i indicates the reduced barrier height of the top i, it is defined as $s_i = 4V_{3,i}/9F_{ii}$.

$$\lim_{s_i \to \infty} \langle v_K \sigma, i | v'_{K'} \sigma, i\rangle = \delta_{v,v'}. \tag{20}$$

We use this approximation in the transformation of the operators from the rho system into the principal axis system in (15). Hence, the resulting matrix is blockdiagonal in v. In the rigid rotor part (19) we also neglect the off-diagonal matrix elements by setting

$$\langle v_K \sigma, i | v'_{K'} \sigma, i\rangle = 0 \quad \text{for} \quad v \neq v' \quad \text{and} \quad K, K' \quad \text{arbitrary}, \tag{21}$$

but for the diagonal terms in v we use the torsional integrals analogous to the formulas given in [18]. If only the truncated Hamiltonian $\hat{H}_{rr} + \hat{H}_1 + \hat{H}_2$ is regarded, like it is mostly done for ground state calculations, no matrix elements off-diagonal in v occur. In this case the dimension of the energy matrix is $2J + 1$.

If top-top coupling terms are introduced, more torsional basis functions have to be used, because the operators $(\hat{p}_i - \varrho_i \hat{P}_{z'})$ and $\sin(3\tau_i)$ introduce large off-diagonal elements in v. The ground state torsional basis function $|v_K = 0\sigma, 1\rangle |v_K = 0\sigma, 2\rangle$ (abbreviated $|0\sigma, 1\rangle |0\sigma, 2\rangle$) is connected with the excited state $|v_K = 1\sigma, 1\rangle |v_K = 1\sigma, 2\rangle$ (or $|1\sigma, 1\rangle |1\sigma, 2\rangle$). Furthermore, a strong coupling between the first excited states $|1\sigma, 1\rangle |0\sigma, 2\rangle$ and $|0\sigma, 1\rangle |1\sigma, 2\rangle$ occurs. Therefore, to calculate the first torsional excited states it is necessary to use the torsional basis functions $|0\sigma, 1\rangle |1\sigma, 2\rangle$ and $|1\sigma, 1\rangle |0\sigma, 2\rangle$. This increases the size of the matrix to $2(2J + 1)$.

In (17) we do not use the fact that $\hat{p}_i$, $\sin\tau_i$ and $\cos\tau_i$ commute with $\hat{D}_i$. Instead we perform the multiplication (18) using the $\hat{D}_i$ operators for all matrix elements obtained in the rho axis systems. Test calculations showed that omission of this transformation for the τ_i dependent operators $\hat{p}_i$, $\cos 3\tau_i$ and $\sin 3\tau_i$ gave worse results compared with the program written by Meyer [17]. Using the transformation, similar results are obtained.

Symmetry and Spin Statistics

The molecular symmetry of trans-2,3-dimethyloxirane is C_2. The operations leaving the Hamiltonian invariant are elements of the direct product group $C_{3v}^- \otimes C_3^+$ [22]. The spin exchange group of the eight hydrogen atoms is also isomorph to $C_{3v}^- \otimes C_3^+$. The nuclear spin of hydrogen ($I = 1/2$) leads to spin statistical weights as given in [23]. Because the torsional state $v_{33} = 1$ is an antisymmetric state, the correlation between the symmetry elements of the Four group (labelled by the odd or even K_- and K_+ quantum numbers) with the species of ${C_{3v}}^- \otimes C_3^+$ is exchanged, as shown in Table 1. The effect of this reversed spin statistics can be seen in Figure 2. It shows the same transition in different torsional states, leading to different intensities for A and E_+ transitions. The G and E_- transitions are not affected.

Measurements and Assignment

The sample of TEB was purchased from Aldrich, Steinheim RFG, and was used without further purification. The spectrum was recorded using our waveguide Fourier transform microwave spectrometers in the range from 8 to 26.4 GHz [24, 25]. The temperature in the cell was kept at about 233 K, the pressure at about 0.05–0.1 Pa. It should be noted that these spectrometers do not utilize a molecular beam. The very low temperature in the beam permits the observation of rotational transitions in the torsional and vibrational ground state only.

Due to its C_2 symmetry TEB has one permanent dipole moment component along the b axis, the magnitude of μ_b was determined by Emptage to 2.04 D [1]. The rotational transitions of TEB in the excited torsional states are generally shifted to lower frequencies compared to the well known ground state lines. The assignment started by identifing the $J_{K-,K+} = J_{1,(J-1)} - J_{0,J}$ transitions by their characteristic tor-

Table 1. Symmetry labels and spin statistical weight factors. σ_1 and σ_1 labels the symmetry of the torsional basis function of top 1 and 2 ($0 = A$, $\pm 1 = E$). e and o designate the even or odd $K_- K_+$ quantum numbers in the rigid rotor limit.

Abbr.	σ_1	σ_2	$C_{3v}^- \otimes C_3^+$	Weight	ee–oo	eo–oe
A	0	0	$A_1 A$	9	$v_{17}=1$	$v_{33}=1$
			$A_2 A$	7	$v_{33}=1$	$v_{17}=1$
E_+	± 1	± 1	$[A_1 E_a + A_1 E_b]$	5	$v_{17}=1$	$v_{33}=1$
			$[A_1 E_a + A_2 E_b]$	3	$v_{33}=1$	$v_{17}=1$
E_-	± 1	∓ 1	EA	4	all states	
G	± 1	0	$[E E_a + E E_b]$	16	all states	
	0	± 1				

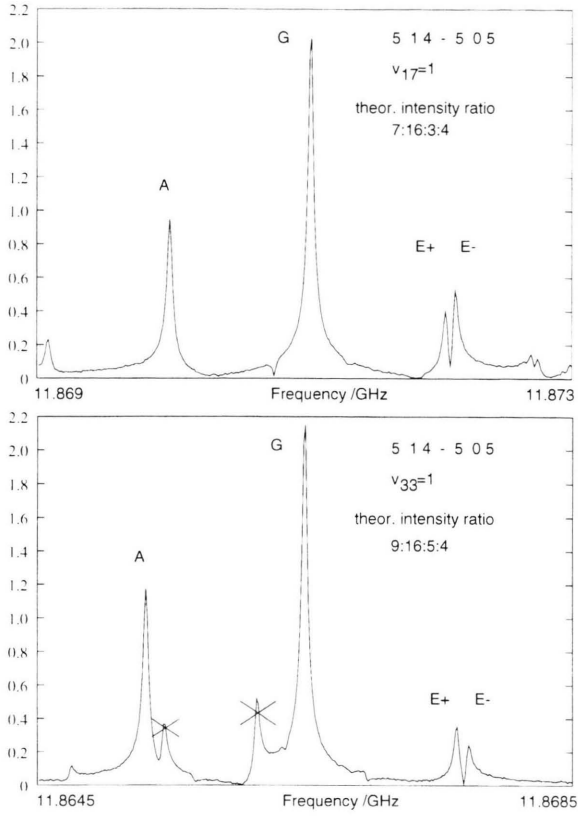

Fig. 2. Rotational transition $J'K'_-K'_+ - JK_-K_+ = 514-505$ in the $v_{17} = 1$ and $v_{33} = 1$ state. The different spin statistical weights in both states can be seen easily at the E_- and E_+ components. Recording temperature 230 K, pressure 0.1 Pa, sampling interval 10 ns, 4 k data points with an additional 4 k zero points prior to the FFT, 6.5 mio. averaging cycles, microwave power 22 dBm, pulse length 300 ns.

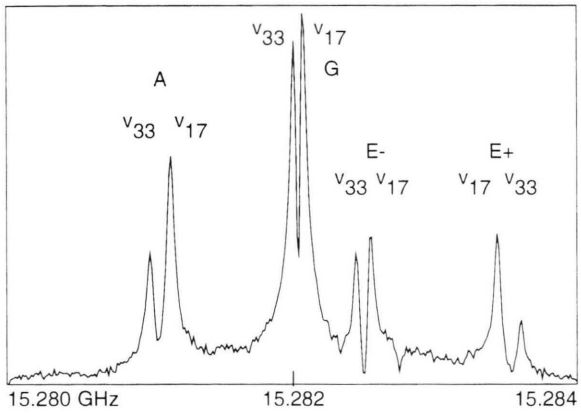

Fig. 3. Rotational transition $J'K'_-K'_+ - JK_-K_+ = 111-000$ in the $v_{17} = 1$ and $v_{33} = 1$ state. Recording temperature 230 K, pressure 0.1 Pa, sampling interval 10 ns, 4 k data points with an additional 4 k zero points prior to the FFT, 6.5 mio. averaging cycles, microwave power 22 dBm, pulse length 300 ns.

sional fine structure pattern influenced by spin statistics. The magnitude of the splitting is about a factor of 30 larger than in the ground state. Because the differences $A-C$ of the rotational constants A and C in both excited states are very similar, the respective b-type transitions with low J appear at almost the same frequency (see Figure 3). Using the known angles between the internal rotation axes i and the principal axes g for the ground state it was possible to do an initial fit of the V_3 and V'_{12} values. With the resulting predictions the other transitions were assigned easily. The list of observed transitions is given in Table 2. The symmetry species are abbreviated A, G, E_+ and E_-. The correlation of these species to the species of the invariance group $C^-_{3v} \otimes C^+_3$ of the Hamiltonian is given in Table 1.

We used the A species of each transition to calculate the rotational constants and centrifugal distortion constants of each state (Table 3). To keep correlations small, the fitted parameters are linear combinations of the rotational constants:

$$B_J = (B + C)/2\,, \quad B_K = A - (B + C)/2\,,$$
$$B_- = (B - C)/2\,. \tag{22}$$

Since correlation coefficients are unreliable in the case of more than two parameters [26], the dependencies of the parameters in the fit are represented by the freedom values given in Tables 3 and 4. Additionally, two correlation matrices are shown. A small freedom value indicates a highly correlated parameter, a freedom value of unity means no correlation. The rotational constants in Table 3 were calculated taking the internal rotation into account, they are not the rotational constants of a rigid rotor applied to the A lines. So they can be regarded as the structural rotational constants for this torsional state.

To distinguish between the v_{17} and the v_{33} torsional state the spin statistics gave us very helpful hints. The spin statistical intensities allowed to distinguish both states clearly. It turned out, that the symmetric v_{17} torsional state is below the antisymmetric v_{33} state, because the $v_{17} = 1$ transitions show a little higher intensities in the spectrum.

Internal Rotation Analysis

The internal rotation of the two equivalent methyl-groups leads to a splitting of the rotational transitions into four components labeled A, G, E_+ and E_-. Be-

Table 2. Observed transitions (in MHz) of trans-2,3-dimethyloxirane. Heading (a) corresponds to the A transitions, heading (b) to the G, E_+, and E_- transitions. Γ: symmetry species of Table 1. $\Delta\nu = \nu_{Sym} - \nu_A$. δ shows the (observed − calculated) values for fit 1.

$J'K'_-K'_+ JK_-K_+$ (a) Γ (b) Γ	ν $\Delta\nu$	$\delta\nu$ $\delta\Delta\nu$	ν $\Delta\nu$	$\delta\nu$ $\delta\Delta\nu$
	$v_{17}=1$		$v_{33}=1$	
110–101 A	9139.390	−0.001	9140.880	0.003
– G	1.366	0.002	1.565	−0.009
– E_+	2.273	0.001	2.548	−0.021
– E_-	3.176	−0.005	3.731	0.005
111–000 A	15281.112	0.004	15280.968	−0.004
– G	0.938	0.008	1.009	−0.009
– E_+	2.309	−0.006	2.621	0.004
– E_-	1.416	0.009	1.451	−0.009
211–202 A	9499.588	−0.002	9500.326	0.004
– G	1.206	0.003	1.360	−0.011
– E_+	2.269	0.015	2.541	−0.007
– E_-	2.565	0.007	2.927	−0.008
212–101 A	21422.821	0.000	21421.059	−0.003
– G	1.106	0.002	1.234	−0.002
– E_+	2.350	−0.007	2.666	0.001
– E_-	2.066	0.010	2.276	−0.004
312–303 A	10058.934	−0.002	10058.451	−0.002
– G	1.153	0.004	1.300	−0.004
– E_+	2.222	0.002	2.502	−0.009
– E_-	2.289	0.015	2.705	0.000
303–212 A	10984.309	−0.002	10974.618	0.004
– G	−1.031	−0.007	−1.148	−0.002
– E_+	−2.211	−0.013	−2.487	−0.002
– E_-	−1.910	−0.012	−2.107	−0.006
321–312 A	25900.714	−0.005	25908.150	0.002
– G	8.875	0.004	10.650	0.006
– E_+	6.818	0.010	7.674	−0.023
– E_-	24.668	−0.008	29.311	0.021
413–404 A	10839.682	0.003	10837.427	−0.001
– G	1.103	−0.003	1.248	−0.005
– E_+	2.160	−0.004	2.458	0.011
– E_-	2.267	0.009	2.571	0.005
422–413 A	25315.864	0.004	25324.223	0.003
– G	5.380	0.000	6.349	−0.004
– E_+	6.797	0.003	7.662	−0.020
– E_-	14.443	0.010		
432–523 A	12063.912	0.001	12086.109	0.000
– G	−20.648	0.008	−23.539	−0.005
431–524 A	12420.489	0.000	12441.173	0.000
– G	31.701	−0.002	35.990	−0.025
514–505 A	11869.967	−0.001	11865.285	0.000
– G	1.085	0.002	1.191	−0.004
– E_+	2.076	−0.002	2.337	−0.012
– E_-	2.156	0.012	2.438	0.005
505–414 A	24914.307	0.000	24898.633	−0.002
– G	−1.033	−0.003	−1.165	−0.005
– E_+	−2.120	−0.022	−2.380	−0.008
– E_-	−2.019	0.000	−2.274	−0.004
514–423 A	8123.308	0.001	8101.054	0.001
– G	−1.355	−0.011	−1.226	0.013
– E_+	−6.740	−0.017	−7.596	0.006
– E_-	1.030	−0.031	2.239	0.039
523–514 A	24667.338	−0.001	24676.515	−0.002
– G	4.233	0.004	4.898	−0.001
– E_+	6.761	0.010	7.619	−0.014
– E_-	10.137	0.002	11.933	0.003

cause TEB has a high barrier to internal rotation, the resulting pattern is split several megahertz only, and the internal rotation is clearly separable from the rigid rotor Hamiltonian describing the absolut position of the pattern itself. Because TEB is an only slightly asymmetric top, the energy levels of the high K_- quantum numbers are almost equal. The internal rotation perturbation on these nearly degenerate levels leads to strong effects, consequently, relatively wide splittings of the high K_- transitions can be observed.

To determine the internal rotation parameters we used the differences $\Delta\nu$ of the frequencies ν between the A and the other three components only. This procedure has two advantages: (i) the splittings $\Delta\nu$ are strongly dependent from the internal rotation parameters but less dependent from the rotational constants, (ii) the standard deviation of this fit shows directly the accuracy of the internal rotation model used here. A global fit instead, mixes the internal rotation model and the centrifugal distorted rotor model (Watson A reduction), and the differences between the observed and calculated values for each frequency contain the errors of both. No distinction between both models can be made in this case. It should be mentioned that a separation between the internal rotation splittings and the absolut frequencies described by a rigid rotor is only true in the case of a high barrier V_3. For low barriers, only a global fit is possible.

At first we fitted the splittings of the first excited torsional states $v_{17}=1$ and $v_{33}=1$ (see Table 1). We used the torsional basis functions $|0\sigma,1\rangle|1\sigma,2\rangle$ and $|1\sigma,1\rangle|0\sigma,2\rangle$, where 0 or 1 is the torsional quantum number v of the first or second top. No symmetry adaptation according to the equivalent tops was used. We fitted the moments of inertia $I_{\tau,1}=I_{\tau,2}$ of the two methyl groups, the potential parameters V_3 and V'_{12}, and the angles between the internal rotor axes and the principal axes. Because the three angles of one top are not independent, since $\lambda_x^2+\lambda_y^2+\lambda_z^2=1$, we choose the polar coordinates δ and ε to describe the position of the internal rotor axis in the principal axes system. This is analogous to the definition of β and γ for the position of the vector ϱ in the principal axes system.

$$\cos\delta_i = \cos\angle(z,i) = \lambda_{z,i} \quad \text{and}$$

$$\cos\varepsilon_i = \frac{\operatorname{sign}(\lambda_{y,i})\,\lambda_{x,i}}{\sqrt{\lambda_{x,i}^2+\lambda_{y,i}^2}}. \tag{23}$$

For each iteration the parameters β_i and γ_i, which are essential in the CAM, are calculated from the varied δ_i

Table 3. Rotational and centrifugal distortion constants of trans-2,3-dimethyloxirane (Watson A reduction), I^r). $B_J = (B + C)/2$, $B_K = A - (B + C)/2$, $B_- = (B - C)/2$. n: number of observations. σ standard deviation of the fit. F: Freedom parameters (see [26]). The revised ground state constants are obtained from the measurements of [2].

		Ground state	F	$v_{17} = 1$	F	$v_{33} = 1$	F
B_J	GHz	3.24766082(20)	0.09	3.2458469(6)	0.25	3.2446802(7)	0.25
B_K	GHz	8.98978028(53)	0.10	8.9659539(15)	0.23	8.9679948(17)	0.23
B_-	GHz	0.17534682(10)	0.30	0.1752891(12)	0.10	0.1747290(13)	0.10
Δ_J	kHz	0.6021(17)	0.01	0.619(16)	0.22	0.588(17)	0.22
Δ_{JK}	kHz	−1.5185(174)	0.01	−1.630(90)	0.39	−1.475(100)	0.39
Δ_K	kHz	34.0985(58)	0.05	33.782(94)	0.25	33.136(105)	0.25
Δ_j	kHz	0.0825(4)	0.11	0.083(8)	0.26	0.091(9)	0.26
Δ_k	kHz	0.9758(257)	0.04	1.470(560)	0.11	1.670(624)	0.11
σ	kHz	4.6		3.5		3.9	
n		59		15		15	
		Derived parameters					
A	GHz	12.2374411(4)		12.2118006(18)		12.2126750(20)	
B	GHz	3.4230076(2)		3.4211360(14)		3.4194093(15)	
C	GHz	3.0723140(3)		3.0705578(14)		3.0699512(15)	
κ		−0.92347		−0.92089		−0.92356	

Correlation matrix of the parameters from the $v_{17} = 1$ fit. The corresponding matrix of the $v_{33} = 1$ state is almost identical.

B_J	1.000							
B_K	−0.123	1.000						
B_-	−0.003	−0.155	1.000					
Δ_J	0.908	−0.221	0.208	1.000				
Δ_{JK}	−0.014	0.594	0.223	0.135	1.000			
Δ_K	−0.067	0.744	−0.613	−0.244	0.099	1.000		
δ_j	0.032	0.151	0.259	0.016	0.107	0.159	1.000	
δ_k	−0.022	−0.215	0.926	0.190	0.173	−0.681	−0.108	1.000

and γ_i, values. The derivatives of the frequencies to the fitted parameters were obtained numerically by a difference quotient.

Since only the splittings are used as input data, the absolute frequencies and therefore the rotational constants are of inferior importance for the fit. We fixed the rotational constants to the value of the ground state. Furthermore, we assumed that the angles δ_i and ε_i are equal for both torsional states. The C_2 symmetry of the molecule leads to the following relation for the $\lambda_{g,i}$ values of both tops (see Fig. 5 of [2]):

$$\lambda_{a,1} = -\lambda_{a,2}\,, \quad \lambda_{b,1} = \lambda_{b,2}\,, \quad \lambda_{c,1} = -\lambda_{c,2}\,. \tag{24}$$

Using the I^r representation, the following relations for the δ_i and ε_i parameters are obtained.

$$\varepsilon_1 = -\varepsilon_2\,, \quad \delta_1 = 180^\circ - \delta_2\,. \tag{25}$$

The standard deviation of the fit, including 81 observed splittings, is about 12 kHz, at a root mean square splitting of about 5 MHz. All input data have similar experimental errors, because they are measured with the same type of spectrometer. Hence, all frequencies have the same weight in the fit.

In a second fit, we additionally included the ground state transitions from [2] and were able to determine the potential parameter V_6 together with the above mentioned constants. Another additional fit was made with the same input data as fit 1, but we fixed the value of V_6 to the one obtained by fit 2. The results of all three fits are compiled in Table 4.

Discussion

In the present paper we report on an analysis of the torsional excited states in the microwave spectrum of trans-2,3-dimethyloxirane. We successfully utilized the combined axis method (CAM) to fit the internal rotation parameters to the observed splittings and to obtain the potential parameters V_3, V_6, and V'_{12}. In former publications on two top molecules the CAM was used only for the ground state transitions; we now proved that it is also a powerful technique to analyze the microwave spectrum of molecules in torsional excited states. The advantage of the CAM over the principal axes methods diagonalizing a truncated energy

Table 4. Internal rotation constants of trans-2,3-dimethyloxirane. [...]: assumed values. n: number of observations. σ standard deviation of the fit. For freedom parameter F see [26]. [a]: experimental results [5].

		Fit 1	F	Fit 2	F	Fit 3	F
V_3	kJ/mol	10.3650(47)	0.03	10.3956(42)	0.03	10.4086(77)	0.03
V_3	cm^{-1}	866.446(398)		869.006(353)		870.092(640)	
V_6	kJ/mol	[0.0]		−0.2600(12)	0.37	[−2.600]	
V_6	cm^{-1}	[0.0]		−21.730(99)		[−21.730]	
V'_{12}	kJ/mol	−0.39835(66)	0.97	−0.42398(63)	0.95	−0.42441(76)	0.89
V'_{12}	cm^{-1}	−33.300(55)		−35.442(53)		−35.478(63)	
I_τ	$uÅ^2$	3.1975(16)	0.14	3.2117(13)	0.05	3.2077(17)	0.03
δ_1	deg.	23.988(53)	0.12	24.396(50)	0.12	24.332(81)	0.08
ε_1	deg.	62.65(32)	0.89	61.90(29)	0.90	62.29(35)	0.85
σ	kHz	11.7		10.4		12.6	
n		81		235		81	
	Derived parameters						
∠ $(a, 1)$	deg.	23.988(53)		24.396(39)		24.332(81)	
∠ $(b, 1)$	deg.	79.236(139)		78.781(128)		78.956(165)	
∠ $(c, 1)$	deg.	68.831(109)		68.633(103)		68.606(142)	
β_1	deg.	6.533		6.666		6.642	
γ_1	deg.	60.049		59.248		59.669	
F_{ii}	GHz	170.438		169.678		169.883	
F_{12}	GHz	−12.143		−12.064		−12.086	
s		67.73		68.24		68.42	
v_{17}	cm^{-1}			175.8(181.5[a])			
v_{33}	cm^{-1}			203.7(200.0[a])			

Correlation matrix of fit 2

V'_{12}	1.000					
V_3	−0.288	1.000				
V_6	0.018	−0.203	1.000			
I_τ	−0.284	0.986	−0.137	1.000		
ε_i	−0.047	−0.072	−0.038	−0.050	1.000	
δ_i	0.258	−0.895	0.049	−0.829	0.185	1.000

matrix [17] are the reduced computational times, because the size of the matrices on the latter technique is in the range of $36(2J + 1)$, in contrast to $2(2J + 1)$ for the CAM.

Our value for the potential barrier $V_3 = 869.0\ cm^{-1}$ is in agreement with the value of Emptage [1] ($V_3 = 854(52)\ cm^{-1}$). The difference in V_3 is influenced by the inclusion of the excited states in our analysis. Our value of V_3 approaches the value given be Durig et al. ($905.4(36)\ cm^{-1}$) [5]. The parameter V_6 obtained from the presented analysis ($-21.7(1)\ cm^{-1}$) agrees in order of magnitude with Durig's result ($-35.1(19)\ cm^{-1}$). As in the analysis of the low resolution IR- and Raman spectra higher states were included, the difference is not astonishing.

The potential top-top coupling parameter ($V'_{12} = -35.4\ cm^{-1}$) of TEB is smaller compared to 2,2-dimethyloxirane ($V'_{12} = -90.6(15)\ cm^{-1}$) [27] because almost no steric interaction between the methyl group should occur in TEB. The value of V'_{12} of TEB exceeds the value obtained by Durig ($V'_{12} = -10.8\ cm^{-1}$) by a factor of 3. The parameter V'_{12} is mainly determined by the energy difference between the torsional modes $v_{17} = 1$ and $v_{33} = 1$. A calculation of the V'_{12} parameter using only the frequencies of the fundamentals as reported in [5] (see Table 4) yields a value of $V'_{12} = -13.2\ cm^{-1}$. Using our microwave parameters of Table 4, we find that the energy difference of the v_{17} and v_{33} fundamentals should be $29\ cm^{-1}$. The contribution of the kinetic parameter F_{12} to this splitting is about $13\ cm^{-1}$, whereas in our data the potential parameter V'_{12} adds about $15\ cm^{-1}$, but only about $6\ cm^{-1}$ if the IR- and Raman data are used. Ab-initio calculations [28] result in an energy difference of the $v_{17} = 1$ and $v_{33} = 1$ states in the order of 18, 19, and $21\ cm^{-1}$ depending on the choosen basis sets.

In our analysis the magnitude of the contribution of the potential parameter V'_{12} is relatively high, contrary

to our expectation. This may be an indication that the model of a rigid frame and rigid internal rotors is not sufficient here because it is also possible that the shift of 15 cm^{-1}, introduced by the V'_{12} term, includes contributions from interactions with other molecular motions and is not only a consequence of a steric top-top coupling itself.

It would be useful to compare potential parameters of TEB with its isomer cis-2,3-dimethyloxirane, where a stronger top-top coupling should be expected, but unfortunately the microwave data are not presently available. The partial disagreement of the microwave and IR- and Raman data suggests further studies.

Acknowledgements

We thank the members of our group for help and discussion, especially Prof. Dr. A. Guarnieri and Dr. J.-U. Grabow for critically reading the manuscript, and C. Gerke and A. Schwenk for help during the measurements. We also thank the Deutsche Forschungsgemeinschaft, the Fonds der Chemie, and the Land Schleswig-Holstein for funds.

[1] M. R. Emptage, J. Chem. Phys. **47,** 1293 (1967).
[2] H. Hartwig and H. Dreizler, Z. Naturforsch. **47a,** 1051 (1992).
[3] J.-U. Grabow and W. Stahl, Z. Naturforsch. **45a,** 1043 (1990).
[4] U. Andresen, H. Dreizler, J.-U. Grabow, and W. Stahl, Rev. Sci. Instrum. **61,** 3694 (1990).
[5] J. R. Durig, A. B. Nease, and J. J. Rizzolo, J. Mol. Struct. **95,** 49 (1982).
[6] H. Dreizler, Fortschr. Chem. Forsch. **10,** 75 (1968).
[7] R. C. Woods, J. Mol. Spectrosc. **21,** 4 (1966).
[8] R. C. Woods, J. Mol. Spectrosc. **22,** 49 (1967).
[9] H. H. Nielsen, Phys. Rev. **40,** 445 (1932).
[10] B. L. Crawford, Jr., J. Chem. Phys. **8,** 273 (1940).
[11] L. Pierce, J. Chem. Phys. **34,** 498 (1960).
[12] C. C. Lin and J. D. Swalen, Rev. Modern Phys. **31,** 841 (1959).
[13] J. T. Hougen, I. Kleiner, and M. Godefroid, J. Mol. Spectrosc. **163,** 559 (1994).
[14] J. D. Swalen and C. C. Costain, J. Chem. Phys. **31,** 1562 (1959).
[15] A. Trinkaus, H. Dreizler, and H. D. Rudolph, Z. Naturforsch. **28a,** 750 (1973).
[16] W. Bossert, A. Bauder, and H. H. Günthard, Chem. Phys. **39,** 367 (1979).
[17] M. Meyer and H. Dreizler, J. Mol. Spectrosc. **148,** 310 (1991).
[18] J. M. Vacherand, B. P. van Eijck, J. Burie, and J. Demaison, J. Mol. Spectrosc. **118,** 355 (1986).
[19] H. Hartwig, PhD thesis, Universität Kiel, 1996.
[20] R. N. Zare, Angular Momentum, John Wiley & Sons, New York, 1 ed., 1988. Chapt. 3, p. 76.
[21] K. T. Hecht and D. M. Dennison, J. Chem. Phys. **26,** 31 (1957).
[22] H. Dreizler, Z. Naturforsch. **16a,** 1354 (1961).
[23] R. J. Myers and E. B. Wilson Jr., J. Chem. Phys. **33,** 186 (1960).
[24] M. Krüger, C. Gerke, H. Harder, and H. Dreizler, Z. Naturforsch. **48a,** 737 (1993).
[25] T. Köhler and H. Mäder, Mol. Phys. **86,** 287 (1995).
[26] J.-U. Grabow, N. Heineking, and W. Stahl, J. Mol. Spectrosc. **152,** 158 (1992).
[27] H. Hartwig and H. Dreizler, Z. Naturforsch. **47a,** 1063 (1992).
[28] T. M. Black, P. K. Bose, P. L. Polavarapu, L. D. Barron, and L. Hecht, J. Amer. Chem. Soc. **112,** 1479 (1990).